A probabilistic seismic hazard assessment for Sulawesi, Indonesia

Article *in* Geological Society London Special Publications · April 2016

DOI: 10.1144/SP441.6

6 authors, including:

Athanasius Cipta
Australian National University
24 PUBLICATIONS **71** CITATIONS
SEE PROFILE

Rahayu Robiana
geological agency of indonesia
12 PUBLICATIONS **10** CITATIONS
SEE PROFILE

Jonathan Griffin
Geoscience Australia
32 PUBLICATIONS **104** CITATIONS
SEE PROFILE

Nick Horspool
GNS Science
37 PUBLICATIONS **242** CITATIONS
SEE PROFILE

A probabilistic seismic hazard assessment for Sulawesi, Indonesia

A. CIPTA[1,2]*, R. ROBIANA[1], J. D. GRIFFIN[3], N. HORSPOOL[3], S. HIDAYATI[1] & P. CUMMINS[2,3]

[1]*Geological Agency of Indonesia, Jalan Diponegoro No. 57, Bandung 40122, Indonesia*

[2]*Australian National University, Research School of Earth Sciences, Building 142, Mills Road, Canberra, ACT 0200, Australia*

[3]*Geosicence Australia, Cnr Jerrabomberra Avenue and Hindmarsh Drive, Symonston, ACT 2609, Australia*

**Corresponding author (e-mail: wamditanka_santee@yahoo.com)*

Abstract: A probabilistic seismic hazard assessment that includes the effect of site amplification is undertaken for the island of Sulawesi, Indonesia. High seismic activity rates, both along fast-slipping crustal faults including the major Palu-Koro–Matano Fault System and in regions of distributed deformation, contribute to moderate–high earthquake hazard over all but the SW part of the island. Of particular concern in terms of seismic risk are the numerous cities sited on soft sedimentary basins that have formed due to movement along presently active structures and that can be expected to amplify earthquake ground motions, including the provincial capitals of Palu and Gorontalo.

The island of Sulawesi is actively deforming and experiences frequent seismicity in all but the most SW part of the island. Although mass casualty (1000+ fatalities) earthquake events have not previously occurred, more-frequent smaller disasters regularly cause smaller numbers of fatalities and economic losses. The most severe historical event in terms of fatalities is the Toli-toli earthquake and tsunami (M_s 7.4, 1968, as in Pelinovsky *et al.* 1997) that killed 200 people (BNPB 2010). Steep topography both onshore and offshore means that landslide is a major secondary hazard, with the extension of faults offshore meaning there is potential for earthquake- and mass-movement-generated tsunami associated with earthquakes. Characterizing earthquake sources and the seismic hazard due to ground shaking is therefore an important step in understanding better the threat from earthquakes faced by the more than 17 million people (BPS 2010) who inhabit the island of Sulawesi.

Hazard maps resulting from this assessment were published by the Geology Agency of Indonesia (Badan Geologi) for the six provinces comprising the island of Sulawesi. The purpose of these hazard maps is to inform resilient building design, local spatial planning and the development of local disaster management plans. In order to be appropriate for these purposes, it is important that the effect of local site conditions on seismic hazard is considered. Site amplification is correlated with local surface geology, and therefore site amplification factors are estimated using proxy methods based on surface geological and morphological data. Furthermore, results are expressed both in terms of spectral acceleration for different periods of ground motion and as felt intensities – with the former being more appropriate for informing building practices, and the latter providing a simpler description of hazard to inform spatial planning and local disaster management planning.

This paper first provides a brief review of the geology and seismotectonics of the island of Sulawesi, and the implications for seismic hazard assessment. Secondly, details of the hazard assessment methodology, the Earthquake Risk Model (EQRM) software package and input parameters used in the model are described. A key aspect is a comparison of suitability of the site class proxy methods of Matsuoka *et al.* (2006) and Wald & Allen (2007) for estimating amplification due to local site effects. In the final part of the paper, the hazard assessment results are presented and discussed.

Geological and seismotectonic setting

The island of Sulawesi consists of a number of fragments of lithosphere that display a complex geological history of subduction, collision and local extension (Fig. 1). West Sulawesi, including the southern arm, is underlain by relatively strong, thick and cool lithosphere that was rifted from Australia and accreted to Sundaland in the Cretaceous (Hall 2011). The SE and east arms are derived

From: CUMMINS, P. R. & MEILANO, I. (eds) *Geohazards in Indonesia: Earth Science for Disaster Risk Reduction*. Geological Society, London, Special Publications, **441**, http://doi.org/10.1144/SP441.6

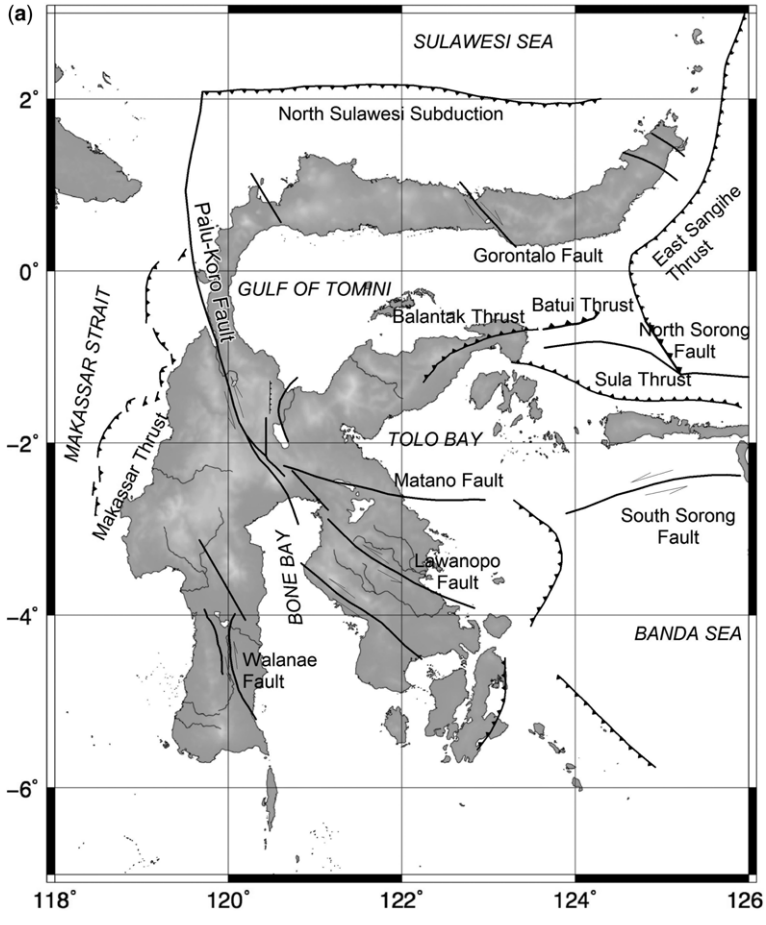

Fig. 1. Map of (**a**) the main active fault structures of the Sulawesi region.

from fragments of continental Australia (Sula Spur) that were accreted during the Miocene; the north arm represents a volcanic arc formed by north-dipping subduction in the early Miocene and associated thrusting of ophiolites onto the Sula spur during collision (Silver *et al.* 1983*a*; Hall 2011). Subduction polarity of the north arm has reversed and now the Celebes Basin subducts southwards beneath the north arm at the North Sulawesi Trench. Seismicity defines a north-dipping slab east of 122.3° E (McCaffrey & Sutardjo 1982 report 122.6 °E) and the south-dipping slab extends deeper west of here.

East of the North Sulawesi Trench there is double-subduction of the Moluccas Sea Plate (Silver & Moore 1978). Active thrust faulting above the Molluccas Sea Plate verges away from the collision zone as frontal arc sediments are overthrust onto the volcanic arc. This area is associated with intense seismic activity both within the slab and on the thrust faults. Deep earthquakes associated with the subducted slabs occur beneath North Sulawesi; there is also a cluster of deep earthquakes that appear to be associated with the enigmatic Una-Una Volcano in the middle of the Gorontalo Basin (Hall 2011). The Gorontalo Basin may represent a zone of extension resulting in the sharp topography changes between the north arm, Gorontalo Basin and Central Sulawesi (Hall 2011). Furthermore, low-angle detachment zones have been identified in the Tokorondo and Pompangeo mountains of Central Sulawesi (Spencer 2011). Thrusting also occurs in the SE along the Tolo Thrust and to the west along the Makassar Thrust. Seismic reflection profiles (Puspita *et al.* 2005) show that the Makassar Thrust is a significant feature that probably extends to meet the Palu-Koro Fault, NW of Palu. This is consistent with horizontal GPS velocities from Sulawesi that,

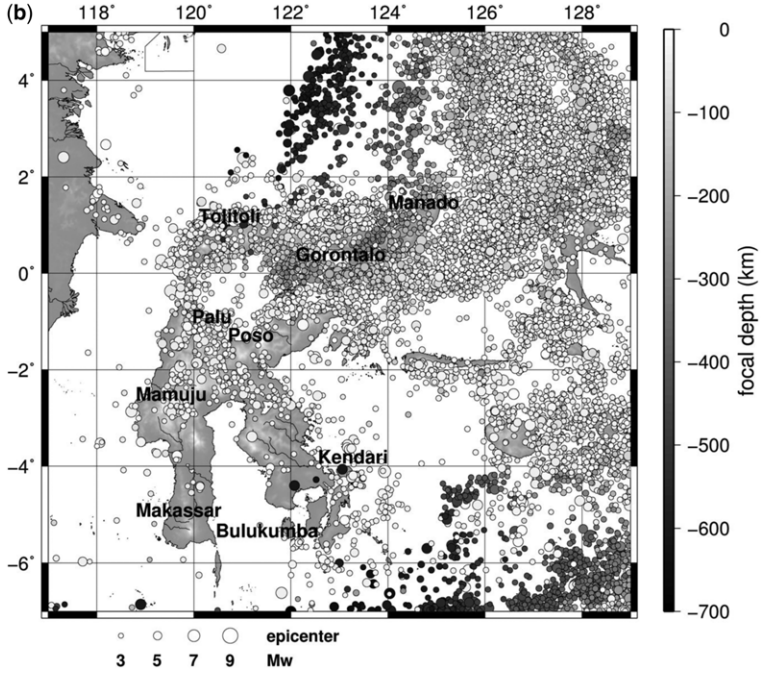

Fig. 1. (**b**) the distribution of earthquake epicentres.

in general, are directed to the NW quadrant with respect to a stable Sunda Block reference frame (Sarsito *et al.* 2011).

Various attempts have been made to interpret Sulawesi into a number of blocks or microcontinents from GPS and gravity anomaly studies (Socquet *et al.* 2006; Sarsito *et al.* 2011). It is unclear how many blocks are needed: however, there are probably more blocks than can be modelled with the available data (D.A. Sarsito pers. comm. 2011). Block boundaries interpreted from GPS measurements match the location of some major mapped faults (e.g. the Palu-Koro Fault and the North Sulawesi Trench), while others are more speculative (e.g. extending from the Poso Fault through the Gorontalo Basin towards the West Molluccas Sea Thrust). Furthermore, Socquet *et al.* (2006) suggested there are four strands of the Palu-Koro Fault that cover an area 50 km wide near Palu. Geological maps from the Geological Agency of Indonesia (Badan Geologi) show a highly faulted landscape, with numerous faults considered active. However, most structures have no information on activity rates or correlation with the GPS block models of Sarsito *et al.* (2011). This makes specific inclusion of individual faults in our hazard model difficult. Hall (2011) suggested that the region is better interpreted as a continuum of weak lithosphere overlying a heterogeneous basement that includes areas of old, relatively strong crust, such as that beneath West Sulawesi. This interpretation poses two particular challenges for how to approach development of an earthquake hazard model for the region:

- Developing a source model that balances inclusion of specific faults with inclusion of background source zones – including only fault sources that accommodate the GPS velocities completely is expected to cause an underestimate of hazard in areas of continuous and distributed deformation, and may overestimate hazard along the mapped faults if unmapped structures are accommodating some of the relative motion. The model presented here includes active fault structures where sufficient information is available, along with distributed source zones in less-well-defined regions, and attempts to balance the seismic moment between fault and background sources based on recorded seismicity.
- Application of ground-motion prediction equations (GMPEs) for different source regions – the heterogeneous basement structure, including both old Sundaland and Australian continental crust, active or recently active island arc settings and obducted oceanic crust, means that large differences in ground-motion propagation can be expected between different geological regions.

A lack of data with which to constrain ground-motion models means that largely default models are chosen.

Methods

The Earthquake Risk Model (EQRM)

The EQRM is an open-source, event-based earthquake hazard and risk calculator developed at Geoscience Australia (Robinson *et al.* 2006; source code freely available from: http://sourceforge.net/projects/eqrm/). The EQRM generated a synthetic earthquake catalogue based on input parameters defining recurrence and geometry properties for earthquake sources. Earthquake recurrence may be defined using either the bounded Gutenberg–Richter model (Youngs & Coppersmith 1985; Kramer 1996) or the characteristic earthquake model (Schwartz & Coppersmith 1984). Sources may be defined using three different geometric representations, being zones, faults or intraslab sources:

- Zone sources are defined by a geographical polygon, and a minimum and maximum depth: synthetic ruptures occur randomly within this zone, with strike and dip randomly sampled from a uniform distribution within a range of values specified by the user.
- Fault sources are rectangular planes defined by the updip surface projection of the fault trace. Synthetic rupture centroids are randomly distributed on the plane, and strike and dip are controlled by the geometry of plane.
- Intraslab sources are defined using the same functionality as fault sources, except now the plane defines the geometry of the dipping slab and individual synthetic events are allowed to rupture at some angle, or range of angles, out of the plane (out-of-dip rupture). This allows for realistic simulation of the variety of earthquake focal mechanisms that occur within subducting slabs. Out-of-dip rupture can also be used to simulate uncertainty in the dip for fault sources.

Inputs

Catalogue and background crustal source zones. The ISC catalogue was downloaded and declustered using the Seisan software package (Ottemöller *et al.* 2011). The catalogue was separated into shallow crustal (depth $\leq$ 35 km), instraslab (depth $>$ 35 km) and megathrust events. The catalogue is considered complete for events magnitudes great than 4.8 and 5.0 for shallow crustal and intraslab earthquakes, respectively. Gutenberg–Richter b values were calculated for crustal and instraslab events using the maximum likelihood method (Aki 1965) and used for all crustal and intraslab source zones, respectively. Activity rates (λm_0) above a minimum magnitude of catalogue completeness (m_0) were calculated based on the average annual number of events above m_0 within each source zone. Crustal earthquakes within 10 km of mapped active faults were assumed to occur on these faults, allowing for hypocentre location errors (Husen & Hardebeck 2010), and therefore were excluded from the background zone analysis. Major crustal-scale faults were used as boundaries for the source zones, including the Palu-Koro and Matano faults. M_{max} for background crustal source zones was set to 7.5, as it is likely that there are large structures capable of earthquakes of this magnitude that are not included in the fault source model. Focal mechanisms from the Global Centroid Moment Tensor (GCMT) catalogue were used to determine faulting type and infer the geometry of fault structures with background zones.

Four background zones were defined. The Northern Sulawesi Zone, bounded to the south and west by the Palu-Koro–Matano Fault System, to the north by the North Sulawesi Trench and to the east by the West Molluccas Sea Thrust. It is characterized by crust that is undergoing high shear strain resulting from clockwise rotation of the Sula Block along the Palu-Koro–Matano Fault System. A number of strike-slip faults are present within the zone, including the Poso and Gorontalo faults, and also eastern strands of the Palu-Koro Fault (Socquet *et al.* 2006). Extension is probably occurring within the Gorontalo Bay (Hall 2011) and this structure may connect the Poso Fault to the Gorontalo Fault and the West Molluccas Thrust. This structure is also used to define a boundary in block model of Sarsito *et al.* (2011). There is also thrusting to the east along the Batui Thrust. The whole area is seismically active, making further delineation of specific structures difficult without more detailed fault studies. The high background activity rate means that a lack of resolution of specific faults should not adversely affect the results of the seismic hazard assessment (Fig. 2).

The West Sulawesi Zone encompasses the seismically active region west of the Palu-Koro Fault and east of the Makassar Thrust. Again, many faults are delineated on geological maps, but there is no information about activity rates.

The SW Sulawesi Zone encompasses the relatively seismically quiet zone along the SW arm of Sulawesi. This area consists of continental crust and is not actively deforming. The Walanae Fault crosses this structure but has low reported slip rates (2 mm a^{-1}: Irsyam *et al.* 2010). This fault zone is bounded on the east by the Bone Gulf.

The SE Sulawesi Zone is bounded to the north by the Matano Fault, to the east by the Tolo Thrust and

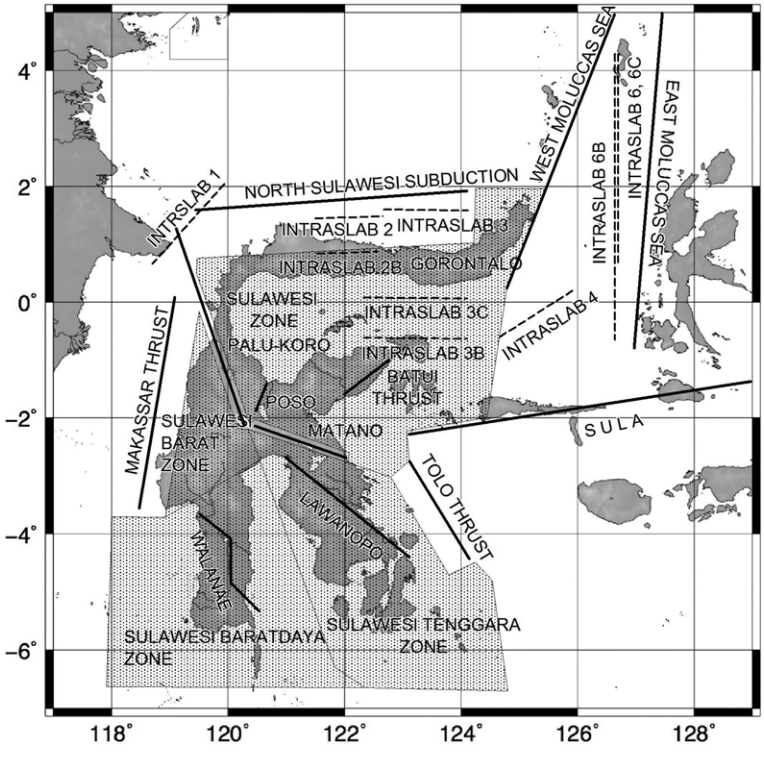

Fig. 2. Fault sources, intraslab sources (updip surface projection of slab trace) and background source zones.

to the west by the Bone Gulf. It is crossed by the Lawanopo Fault. Activity rates here are lower than in the North and West Sulawesi zones.

Fault sources. The initial reference fault model was that used for the 2010 revision of Indonesia's national seismic hazard map (Irsyam *et al.* 2010). However, several of the fault sources were modified to take into account new data regarding fault locations, geometry and earthquake recurrence. Furthermore, where fault sources were located within background source zones (rather than defining the zone boundary), fault-source slip rates derived from geological or geodetic methods (S_g) were reduced by the equivalent slip rate from the activity rate of the background source model. Slip rate (S) can be related to seismic moment rate (M^T) by (Youngs & Coppersmith 1985):

$$M^T = \mu A_f S$$

where A_f is the fault area and μ is the shear modulus. Therefore, the Gutenberg–Richter magnitude distribution, which describes the rate of seismicity and, hence, the seismic moment rate, can be used to relate the slip rate to the seismic activity rate. The background seismicity rate is used to calculate an equivalent slip rate for the fault that lies within it by rearranging from Youngs & Coppersmith (1985):

$$S_\lambda = \frac{b\lambda^f_{m_o} M_o^{max-\beta(m_{max}-m_0)}}{\mu A_f (c-b)(1-e^{-\beta(m_{max}-m_0)})}$$

where S_λ is the estimated slip rate for the fault derived from background seismicity only, M_o^{max} is the moment of the maximum magnitude earthquake (m_{max}) for the background zone, $c = 1.5$ from the moment magnitude definition of Hanks & Kanamori (1979) and $\beta = 2.303$, and $\lambda^f_{m_o}$ is the activity rate of the source zone (μ_{m_0}) scaled by the volume of the 10 km buffer around the fault:

$$\lambda^f_{m_o} = \frac{\lambda_{m_o} V_{buffer}}{V_{zone} - V_{buffer}}.$$

Therefore the final input slip rate for the fault is

$$S = S_g - S_\lambda.$$

Reported slip rates for some faults were lower than that calculated from seismicity, giving a negative value for S and demonstrating the difficulty in characterizing individual faults for seismic hazard assessment within a zone of high shear strain and

seismicity. However, as these faults clearly exist, are active and pose a threat, they are still included with a nominal slip rate of 2 mm a^{-1}, acknowledging that this probably results in an overestimate of total seismic moment rate compared with that derived purely from seismicity (although we cannot be sure owing to the incompleteness of the instrumental catalogue).

Fault input parameters. The fault parameters used in this study are shown in Table 1. A brief summary of the key differences between this paper and Irsyam *et al.* (2010) is given below.

The Minahasa (North Sulawesi) Trench. This fault is mapped at the trench axis, as evident in bathymetry (Silver *et al.* 1983*b*; Irsyam *et al.* 2010). However, although a few thrust events have occurred here, the majority of thrust events are located 50–100 km to the south. Focal mechanisms (Fig. 3) show steeper thrusting in the east (average dip 24°) than in the west (average dip 18°), consistent with Silver *et al.* (1983*b*), who observed a steeper frontal slope in the east in seismic reflection profiles. These data show a shallow-dipping main thrust plane with steeper splay faults in the overriding wedge, including north-dipping

Table 1. *Summary of faults parameters used in this paper and Irsyam* et al. *(2010)*

Fault	Slip rate (mm)		M_{max} (M_w)		Fault type	*A*, *b* values
	Irsyam *et al.* (2010)	This paper	Irsyam *et al.* (2010)	This paper		
North Sulawesi			8.2	8.2	M	4.82, 0.914
Palu-Koro	30 (0.25)	35	7.94	7.9	SS	–, 0.95
	35 (0.50)					
	45 (0.25)					
Poso	2	2	6.93	6.9	SS	–, 0.95
Matano	37 (0.50)	41	7.9	7.9	SS	–, 0.95
	44 (0.50)					–, 0.95
Lawanopo	25	20.3	7.59	7	SS	–, 0.95
Walanae	2	–	7.53	–	SS	–, 0.95
Walanae N	–	1.7	–	6.6	SS	–, 0.95
Walanae M	–	1.7	–	6.6	SS	–, 0.95
Walanae S	–	1.7	–	6.6	SS	–, 0.95
Gorontalo	11	5	7.06	7.6	SS	–, 0.95
Batui	2	2	7.06	7.3	R	–, 0.95
Tolo	9 (0.50)	14	7.94	7.5	R	–, 0.95
	19 (0.50)					–, 0.95
Makassar	4 (0.50)	9	7.46	7.5	R	–, 0.95
	13 (0.50)					–, 0.95
Sula	10	14	7.19	7.7	R	–, 0.95
West Mollucca Sea	13	13	8.47	7.9	R	–, 0.95
East Mollucca Sea	29	29	8.47	8.1	R	–, 0.95
Intraslab 1	–	–	–	–	I	0.690, 1.21
Intraslab 2A (shallow)	–		–	8	I	1.100, 1.21
Intraslab 2B (deep)	–	–	–	8	I	5.200 1.21
Intraslab 3	–	–	–	8	I	1.900, 1.21
Intraslab 3A (shallow)	–		–	8	I	6.080, 1.21
Intraslab 3B (deep)	–	–	–	8	I	6.675, 1.21
Intraslab 4A (shallow)	–		–	8	I	8.125, 1.21
Intraslab 6	–	–	–	8	I	15.575, 1.21
Intraslab 6A (west dipping)	–		–	8	I	12.6, 1.21
Intraslab 6B (east dipping)	–		–	8	I	23.625, 1.21
Background seismicity zone						
Sulawesi	–	–	–	7.5	C	10.825, 0.95
Sulawesi Timur (East Sulawesi)	–	–	–	7.5	C	2.925, 0.95
Sulawesi Barat (West Sulawesi)	–	–	–	7.5	C	1.100, 0.95
Sulawesi Baratdaya (SW Sulawesi)		–	–	7.5	C	0.175, 0.95

Note: M, megathrust; SS, strike-slip fault; R, reverse fault; N, normal fault; I, instraslab, variable mechanism; C, crustal, variable mechanism. In the 'Slip rate' column, the number in the brackets indicates the weight value. A-value, event rate for certain region, describes seismic activity; b-value, tectonic parameter, determined by slope of the frequency-magnitude distribution curve.

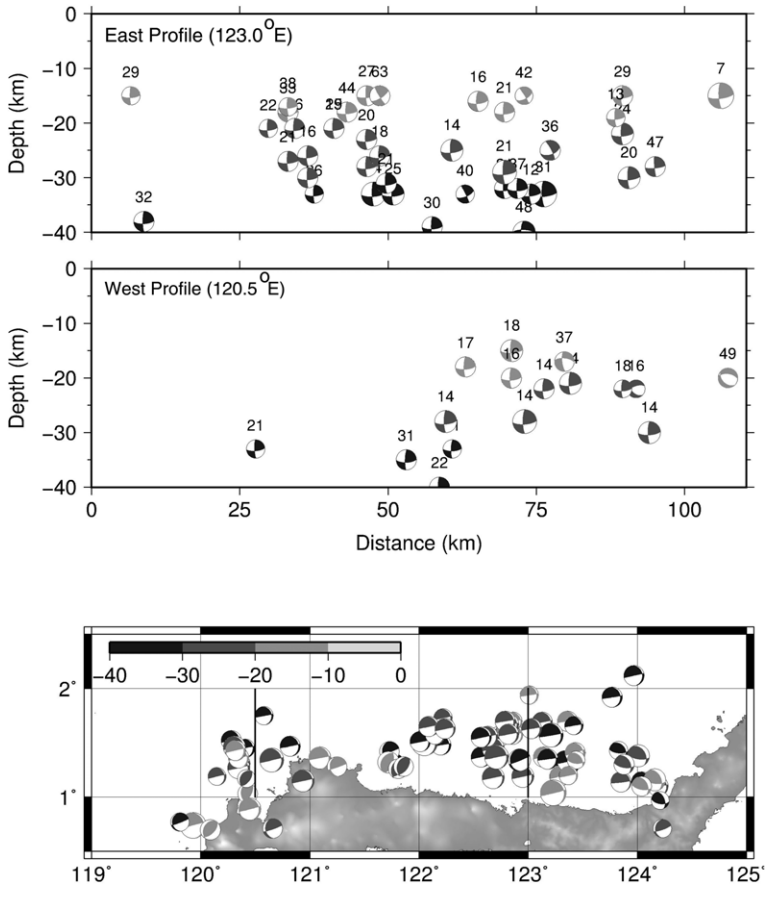

Fig. 3. Focal mechanisms for the Minahasa Trench along north–south profiles showing steeper average dips in the west than in the east. Numbers over each beachball in the upper and middle panels indicate the dip. The area in this figure is indicated by black rectangle in Figure 1a.

structures in the eastern section of the fault (Silver *et al.* 1983*b*).

It is unclear whether the lack of earthquakes near the trench is because strain is not being accumulated within weak sediments (i.e. the theory of Wang & Hu 2006) or if, in fact, these sediments are slowly accumulating strain and could host a large earthquake, as has been observed in the 2004 Great Sumatra–Andaman Earthquake (where there is a thick sedimentary wedge: Gulick *et al.* 2011) and in source models for the 2011 Tohoku, Japan earthquake (Ammon *et al.* 2011; Koketsu *et al.* 2011). If this is the case, then the fault could contain potential to generate a significant tsunami. However, as short-period ground motions generated by subduction interface earthquakes decrease rapidly with distance (e.g. Youngs *et al.* 1997), we place the source fault landwards of the trench axis in order to reproduce, as accurately as possible, the observed seismicity on the main section of the subduction interface. The fault plane is taken to dip at an angle of 21° (mean dip from focal mechanisms): however, synthetic events are allowed to thrust out of this plane by randomly sampling a uniform distribution of dips between 11° and 43°. Events rupturing out of the fault plane are further constrained to extend no more than maximum of 5 km from the fault plane. Fault width is 100 km and the maximum depth is 35 km.

The Batui Thrust. Recent work using high-resolution multi-beam bathymetric and seismic data allowed Watkinson *et al.* (2011) to reassess the tectonics of this region. They found no evidence for the Batui Thrust, as previously mapped to the north of Poh Head (Silver *et al.* 1983*b*; Irsyam *et al.* 2010). Instead, this fault is reinterpreted as occurring as a thrust zone to the SW of the Poh Head peninsula.

We follow this new interpretation of the location of the Batui Thrust. Slip rates from Irsyam *et al.* (2010) of 2 mm a^{-1} are poorly constrained: however, in the absence of further information, we apply this value to the new location of the fault. This rate is lower than that calculated from background seismicity in the surrounding source zone.

The Balantak Fault. This fault is a right-lateral strike-slip structure that cuts Poh Head to the north of the Batui Thrust. It has a clear geomorphic expression and has been associated with recent seismicity (Watkinson *et al.* 2011). This fault is not included in Irsyam *et al.* (2010) and there are no available data on slip rates. Therefore, we do not explicitly include this fault in our assessment.

The Makassar Thrust. Irsyam *et al.* (2010) include this fault offshore of the western bulge of Sulawesi near the city of Majene. We extend this thrust fault to the north to meet the Palu-Koro Fault NW of Palu as seismic reflection profiles (Puspita *et al.* 2005) show clear evidence of thrusting offshore of much of West Sulawesi. It is unclear whether this structure is one continuous structure, as we include it, or a number of segmented thrust faults and fold zones.

Irsyam *et al.* (2010) also identified a number of other active fault structures throughout Sulawesi that were not included in their hazard model owing to a lack of information on slip rates. In addition, the active fault database of the Geological Agency of Indonesia also contains numerous mapped structures, many of which are discernable as topographical lineaments using the SRTM digital elevation model. A lack of geological data and geodetic data to constrain slip rates, and even to confirm the faults are active structures, means that slip rates for individual faults cannot be defined. Therefore, zone sources covering areas of distributed deformation are used instead.

Intraslab sources. Deep seismicity is conspicuous throughout northern Sulawesi, and is the result of a complex system of active and inactive subduction systems, as described above. Although much of the deep seismicity can be explained through these systems, the catalogue also contains some more enigmatic events that are difficult to assign to any structures and suggest a complex pattern of Cenozoic collision that is not fully understood. Identifying structures is further complicated by formal catalogue hypocentre depth uncertainties of up to 25 km (Husen & Hardebeck 2010). We define a number of intraslab sources that attempt to explain the seismicity and fit with geological interpretations of the area.

Table 2. *Ground-motion prediction equations used for each source region and associated logic tree weight*

Region	Ground-motion model	Weight
Crustal	Boore & Atkinson (2008)	0.33
	Campbell & Bozorgnia (2008)	0.34
	Chiou & Youngs (2008)	0.33
Subduction interface	Youngs *et al.* (1997)	0.25
	Atkinson & Boore (2003)	0.25
	Zhao *et al.* (2006)	0.5
Intraslab	Atkinson & Boore (2003) – Cascadia	0.33
	Youngs *et al.* (1997)	0.34
	Atkinson & Boore (2003) – worldwide	0.33

Ground-motion models. At present, ground-motion prediction equations (GMPEs) based on strong-motion data from Indonesia do not exist. At present, work is being started to develop GMPEs from a new strong-motion accelerometer network being deployed by the Indonesian Meteorology, Climatology and Geophysics Agency (BMKG): however, no results are yet available either for Indonesia in general or Sulawesi in particular (Rudyanto 2013). Therefore, we use the logic tree of Irsyam *et al.* (2010), as shown in Table 2.

Site amplification

Amplification of seismic waves in shallow soil near the surface can contribute significantly to variations in seismic hazard between nearby areas exposed to the same seismic sources. To apply site amplification to a regional-scale hazard assessment in Sulawesi where field measurements are limited, proxy methods are used to estimate the average shear-wave velocity in the upper 30 m of the Earth (V_{s30}). Estimated V_{s30} values are then either incorporated directly into those GMPEs that include this term in their functional form or, for those that do not, classified into the NEHRP site classes, and associated amplification factors (Borcherdt 1994) are used to scale ground-motion estimates from the GMPEs at each site.

Two proxy methods for estimating V_{s30} are compared against field measurements of the response spectral ratio of horizontal and vertical components (H/V) of ambient noise measurements. The first proxy method is that of Wald & Allen (2007). This method estimates V_{s30} based purely on topographical slope using empirical relationships derived from data from California and Taiwan. Global SRTM topography has been used to generate

a global grid of V_{s30} using this method, which is freely available online from the United States Geological Survey's Global V_{s30} Server.

The second proxy method follows Matsuoka *et al.* (2006) and estimates V_{s30} as an empirical function of geomorphology, elevation, slope, and the distance from hills and mountains. Empirical factors are derived from analysis of field measurements from Japan. The classification of geomorphology for this method is shown in Table 3. Geomorphological and geological maps held by the Geological Agency of Indonesia (1:250 000 scale, 1973–98) were used along with SRTM topography data to classify Sulawesi's geomorphology using the scheme (ABC) of Matsuoka *et al.* (2006) and then to calculate the V_{s30} estimates.

Sulawesi can be divided into 14 geomorphic units using the Matsuoka *et al.* (2006) scheme. Of these, the classes of Pre-Tertiary mountain, Tertiary mountain, hill, mountain footslope, volcanic footslope and volcano cover more than 75% of the island's area. These classes of geomorphic units are characterized as being in steep and elevated areas subject to erosion, where the ground surface is assumed to be composed of hard and compacted material with high average V_{s30} values. V_{s30} is lower for volcanic than non-volcanic mountains, a key distinction that is useful for application in Indonesia. The remaining 25% of Sulawesi Island is characterized by more undulating or flat morphology where sediments are accumulating.

Figure 4 shows the geomorphology of Sulawesi using the classification of Matsuoka *et al.* (2006) and V_{s30} values derived from empirical relationships. Mountainous regions are characterized by high V_{s30} values (NEHRP site class A or B), footslopes and volcanic areas have moderate V_{s30} values (site class C), while lowland areas (valley, delta and coastal) have lower V_{s30} values and are classified as site class D or E.

Estimated V_{s30} values taken from both the Wald & Allen (2007) and the Matsuoka *et al.* (2006) methods are compared with V_{s30} calculated from ambient noise field measurements in the cities of Gorontalo, Palu and Manado. Measurement locations were classified as volcanic footslope, mountain footslope, delta and coastal lowland, and valley bottom lowland in the Matsuoka *et al.* (2006) scheme.

Field measurements were performed using single-station three-component 1 Hz L4–3D seismometers. Noise was recorded for approximately 20 min and the spacing between measurements was 1–2 km. The fundamental frequency of the ratio of horizontal to vertical components (H/V)

Table 3. *Geomorphological unit classification*

Slope (°)	Elevation (m)	Lithology	Geomorphological unit (Matsuoka *et al.* 2006)	Notes
>15	>700	Tertiary rock	Tertiary Mountain	
		Pre-Tertiary rock	Pre-Tertiary Mountain	
	<700	Tertiary products	Hill	
		Volcanic (Q)	Volcanic Hill	Volcanic product
5–15			Mountain footslope	
		Volcanic (Q)	Volcanic footslope	Volcanic product
≤5		Alluvium, colluviums, fluvial etc.	• Valley bottom lowland • Alluvial fan • Back marsh • Abandoned river channel • Delta and coastal lowland • Marine sand and gravel bars	Colluviums Fluvial
Active volcano			Volcano	Eruption centres
Terrace			• Rocky strath terrace • Gravelly terrace	• Brecciated, geological structure • Alluvium, geological structure
		Volcanic ash	Terrace covered by volcanic ash soil	Volcanic ash
5–15		Sand (Q)	Sand dune • Reclaimed land • Filled land • Natural levee	Sand • Engineered • Engineered • Natural barrier parallel to river/coast, sand bar, flood plain

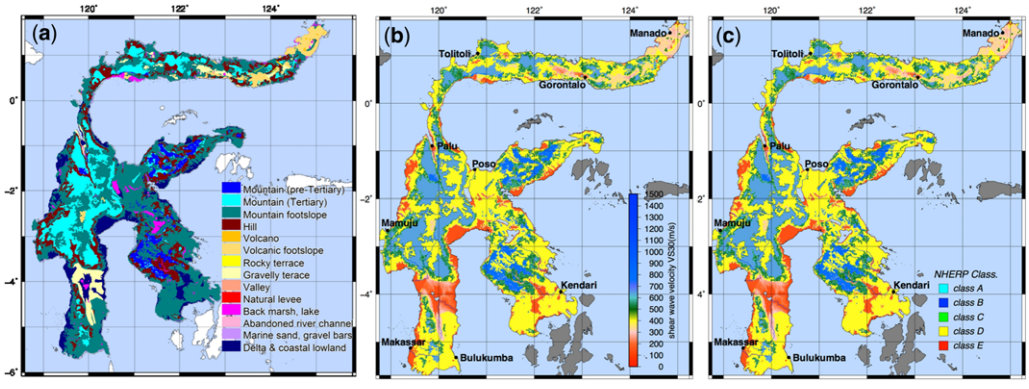

Fig. 4. (**a**) Geomorphology of Sulawesi using the Matsuoka *et al.* (2006) classification, (**b**) V_{s30} values for Sulawesi derived from the Matsuoka *et al.* (2006) method (higher V_{s30} values are indicated in blue and lower V_{s30} values are indicated in red (right)) and (**c**) NEHRP's soil classification.

was determined using Geopsy processing software and then used to estimate V_{s30} following Zhao (2011). This method uses the relationships $T_{V_{s30}} = 120/V_{s30}$, where $T_{V_{s30}}$ is the site period assuming bedrock is reached at a depth of 30 m. In using this method, we assume that site period and V_{s30} are correlated, and that the fundamental period of the H/V ratio is equivalent to $T_{V_{s30}}$. V_{s30} values are then classified into NEHRP site classes (Borcherdt 1994). We note that there is a large degree of uncertainty inherent both in the assumption of the correlation between fundamental period and V_{s30}, and in the application of V_{s30} itself as a predictor of site effects. Overall, the method is more robust for shorter site periods (Zhao 2011).

Figure 5 shows histograms of the difference between V_{s30} values estimated using proxy methods and those based on field measurements. Both proxy methods estimate higher V_{s30} values that those derived from H/V measurements, although the United States Geological Survey (Wald & Allen 2007) method overestimates (222 ± 212 m s^{-1}) by about twice that of the Matsuoka *et al.* (2006) method (102 ± 194 m s^{-1}).

In terms of site classification, higher estimates of V_{s30} using the Wald & Allen (2007) method means that this method is more likely to correctly assign site class C, while the Matsuoka *et al.* (2006) method is more likely to correctly assign site class D (Fig. 6). The Matsuoka *et al.* (2006) method gives the same site class as that derived from H/V measurements (Zhao 2011) at approximately 25% of the measured locations compared with the Wald & Allen (2007) method, which gives the same site class at 15% of the measured sites.

In general, both the Matsuoka *et al.* (2006) and Wald & Allen (2007) methods result in higher estimates of V_{s30} compared with H/V measurements. Weathering is one possible explanation for this difference as the degree of weathering is not taken into account in the proxy methods. For a tropical country like Indonesia, high rainfall levels mean that weathering rates can be much higher than the regions where these proxy methods where derived (Japan and California). This can create deep weathering profiles. It can be said that a wetter climate is prone to faster weathering. Physical weathering breaks the original rock down into soil-like material and, consequently, highly weathered rock loses its engineering properties significantly. Furthermore, clay minerals introduced by weathering reduce effective shear strength and, hence, the shear-wave velocity (Arikan & Aydin 2012).

Hazard modelling results

Probabilistic seismic hazard results are shown for annual probabilities of exceedance of 0.002 and 0.0004 (equivalent to return periods of 500 and 2500 years), and were produced for response spectral acceleration (RSA) of 0.2 and 1.0 s, and peak ground acceleration (PGA). These results are shown in Figure 7, including site amplification. The hazard maps show high hazard in all but the south arm of Sulawesi. Hazard is highest along the Palu-Koro, Matano and Lawanopo faults, where slip rates are greater than 30 mm a^{-1}.

Hazard results by region

North arm. Earthquake hazard in the northern arm of Sulawesi is controlled by the North Sulawesi Subduction Zone and associated intraslab sources to the north, with an additional hazard from intraslab sources to the east of the arm. At longer

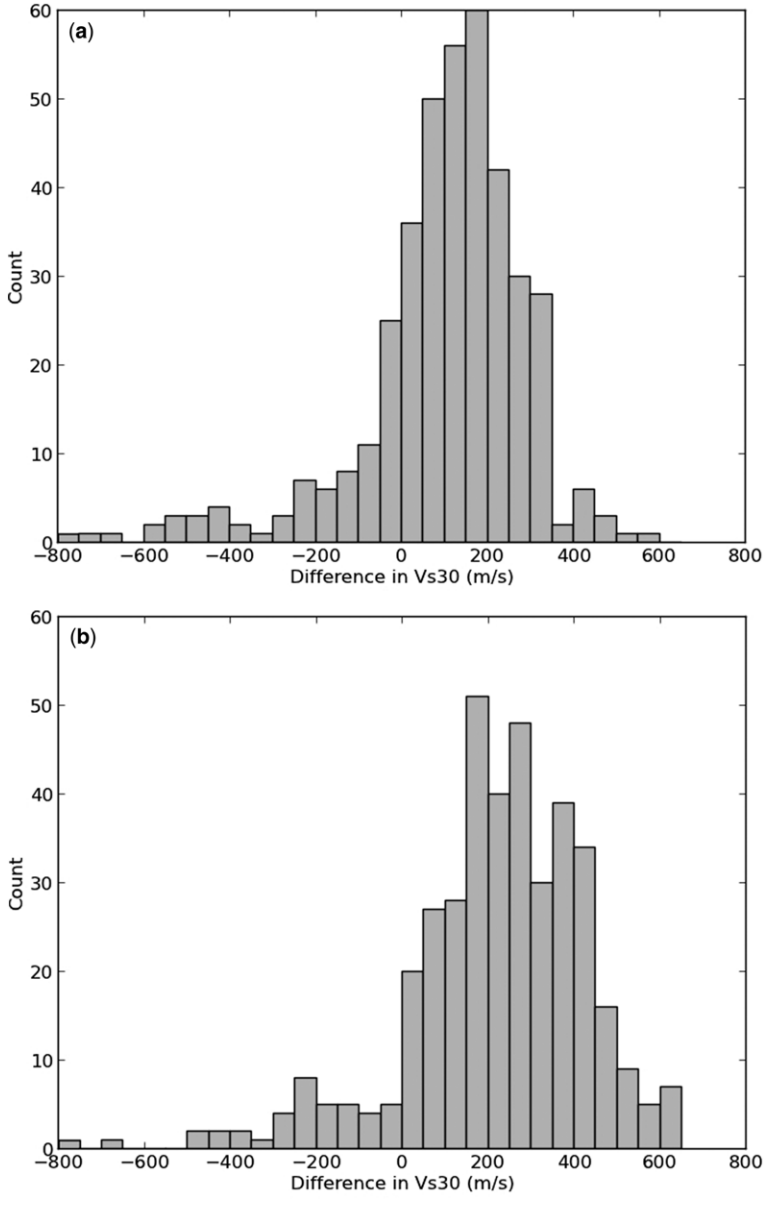

Fig. 5. Histogram of differences in V_{s30} values for (**a**) the Matsuoka *et al.* (2006) method minus H/V-derived measurements, and (**b**) the United States Geological Survey (Wald & Allen 2007) method minus H/V-derived measurements.

return periods (1000 and 2500 years), the Gorontalo Fault contributes significantly to the hazard level. Although the frequency of large earthquakes occurring on the Gorontalo Fault is lower than for other source regions, when these events do occur they can cause high levels of ground shaking as the source is shallow and on land. Earthquake hazard in this area is amplified by soft sediments along the depression created by the Gorontalo Fault, most notably surrounding Lake Limboto between the cities of Limboto (population 50 000) and Gorontalo (population 200 000). Earthquake hazard in the northern arm of Sulawesi is highest in the Buol and Toli-toli districts.

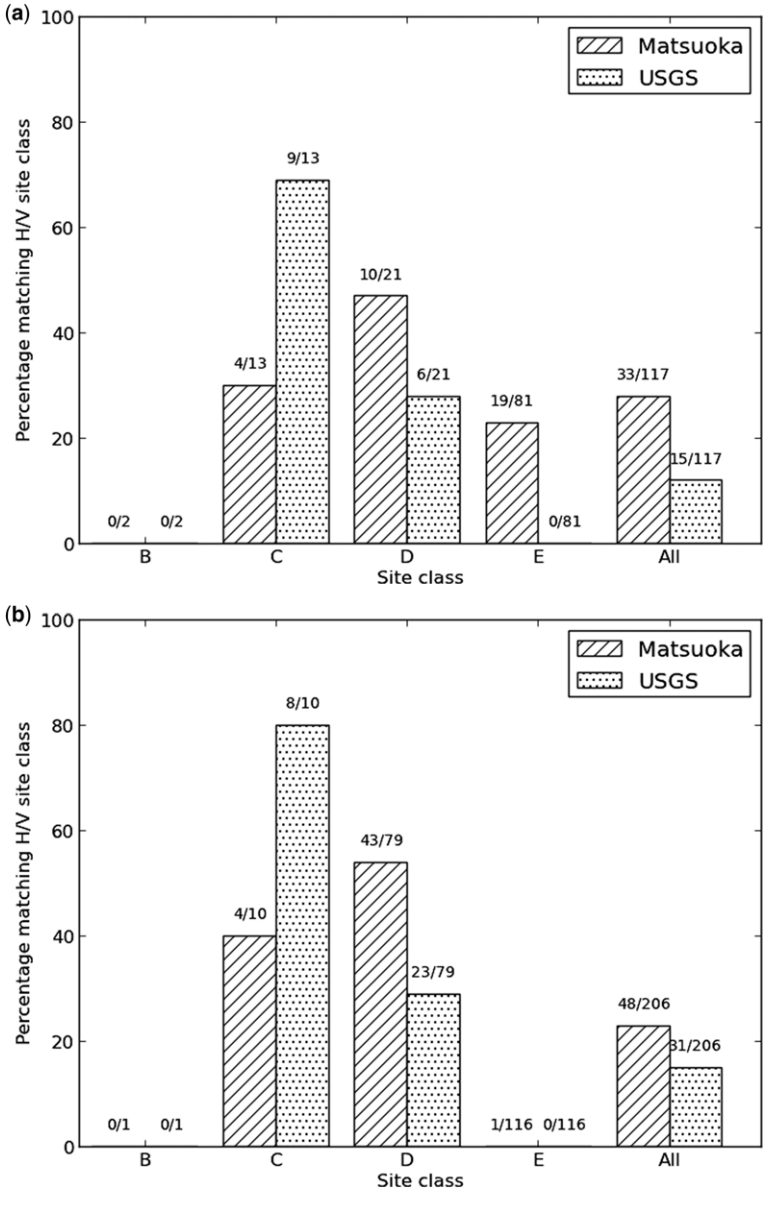

Fig. 6. Comparison of Matsuoka *et al.* (2006) and United States Geological Survey (Wald & Allen 2007) proxy estimates of site class with those derived from H/V measurements using the Zhao (2011) method for (**a**) Palu, (**b**) Gorontalo.

Central and East Sulawesi. Earthquake hazard in Central and East Sulawesi is very high. Hazard is extremely high along fast-moving onshore faults, in particular the Palu-Koro–Matano Fault System and the Balantak–Batui faults. High background seismicity rates drive a high hazard in the area far away from known faults. This pattern is consistent for all return periods and spectral periods simulated. Extremely high hazard (PGA $> 0.8g$ at a 500 year return period) occurs in the city of Palu (population 335 000), located on a pull-apart basin created by strands of the Palu-Koro Fault.

West Sulawesi. Earthquake hazard is generally high in West Sulawesi owing to a high background seismicity rate. Hazard is higher in the east, near the

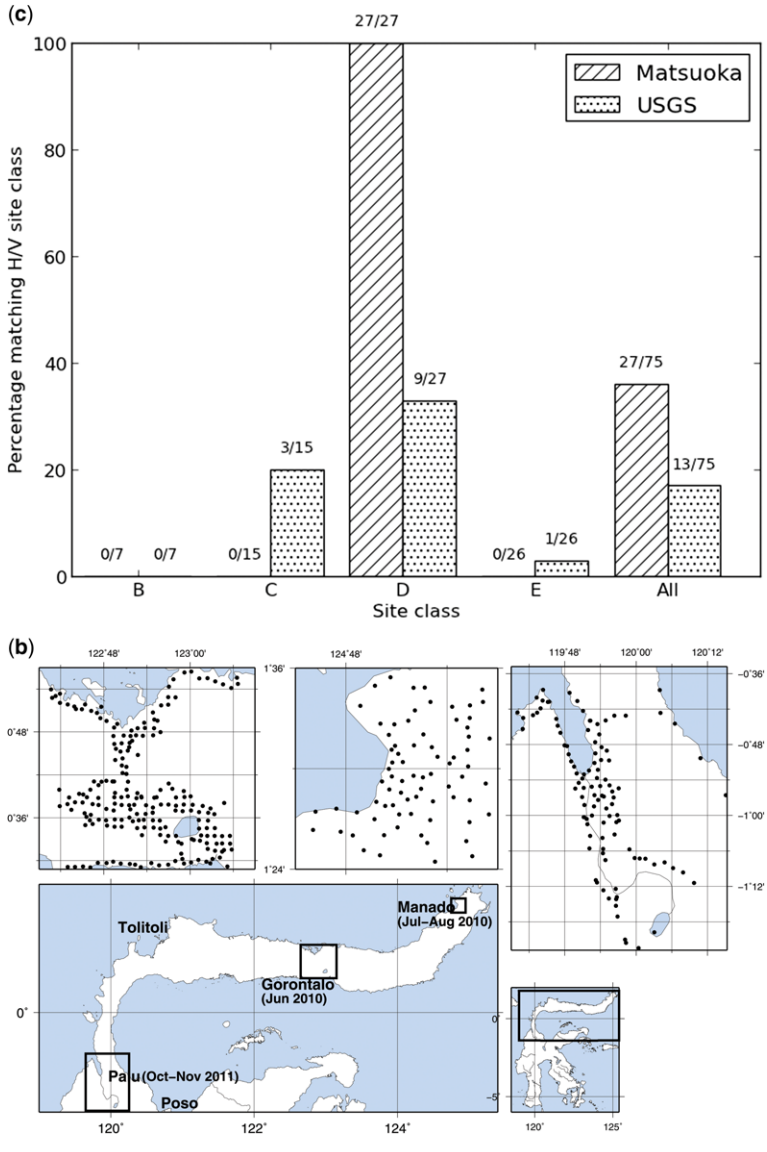

Fig. 6. (**c**) Manado. (**d**) shows measurement points, the year that the measurements were made is written in brackets.

Palu-Koro Fault, and to the west, where the offshore Makassar Thrust is significant.

SE Sulawesi. Earthquake hazard in SE Sulawesi is extremely high along the Matano and Lawanopo faults. The Lawanopo Fault runs just to the north of the city of Kendari (population 200 000), which is sited on a delta and surrounding coastal lowlands (site class E) near Kendari Bay. Background seismicity rates are lower to the south of the Matano Fault. Therefore, to the south of the Matano and Lawanopo faults, earthquake hazard, while still being high, is lower relative to Central and East Sulawesi.

South Sulawesi. Earthquake hazard is high along the Walanae Fault, with lowlands along the depression created by the fault leading to high amplification (site classes D and E) of ground motions. Background seismicity is low, with only a few historical earthquakes recorded in the background zone, and therefore away from the Walanae Fault hazard is

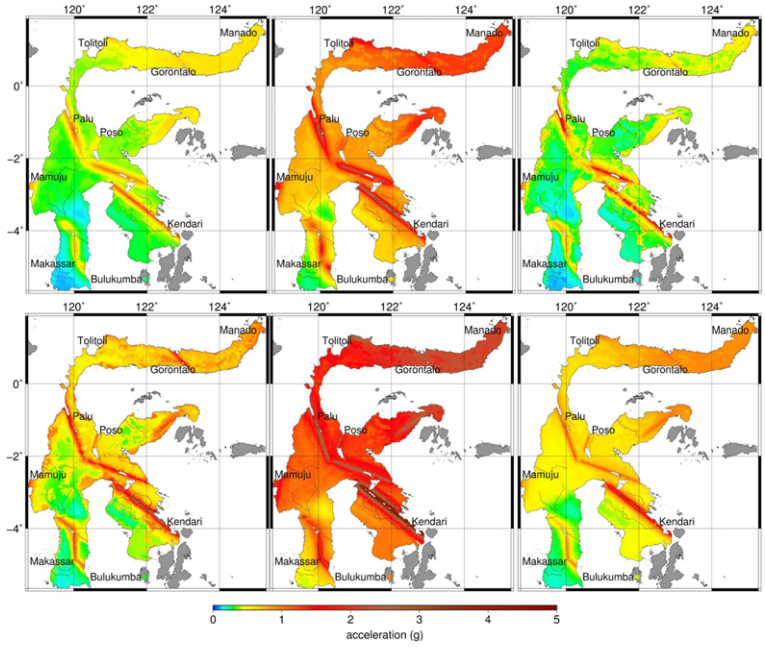

Fig. 7. Peak ground acceleration (PGA) and response spectra (RSA) of 0.2 and 1.0 s for (top) a 500 year return period and (bottom) a 2500 year return period.

much lower than for the rest of Sulawesi. The largest population centre in Sulawesi, Makassar (population 1 340 000), is located in a region of lower hazard relative to the rest of the island.

Using the EQRM, we obtained ground acceleration at each point on a 1 × 1 km grid for all return periods and spectral periods. These results are informative in seismic-resistant building and infrastructure design. For spatial planning purposes at the local scale and for construction of non-engineered buildings, the expected felt seismic intensity is a simpler and more easily communicated measure of hazard. Therefore, in the final step, we convert acceleration to Modified Mercalli Intensity (MMI) using the equation formulated by Atkinson & Kaka (2007) for acceleration at 1.0 s period, including site effects. MMI is then classified into four classes: high hazard zone (MMI $\geq$ VIII); medium hazard zone (MMI VII–VIII); low hazard zone (MMI V–VII); and very low hazard zone (MMI $<$ V) based on the 500 year return period. This is similar to, but slightly different from, the classification of Arya *et al.* (2014).

Comparison against historical data

The conversion of a 500 year recurrence interval 1.0 s hazard to intensity (MMI) is shown in Figure 8 and is overlain with the location of historical damaging earthquakes (Supartoyo & Surono 2008). All historical damaging events occur in regions classified as moderate (four events) or high (30 events) hazard, with the exception of the 1828 Bulukumba earthquake, which occurs in a low hazard region.

Discussion

A probabilistic seismic hazard assessment for the island of Sulawesi, Indonesia, including the effects of site amplification through proxy methods, was undertaken. Much of the island has high hazard, particularly along major, fast-slipping crustal faults, in the highly sheared region north of the Palu-Koro–Matano Fault System and along the north arm of Sulawesi. The SW arm of Sulawesi, including the city of Makassar, is lower hazard compared with the rest of the island, although all regions may experience damaging events at longer return periods. The high hazard regions correlate well with locations of historical earthquake damage, with the exception of the damaging 1828 earthquake in Bulukumba (MMI VIII–IX: Supartoyo & Surono 2008), on the south coast of South Sulawesi, which we speculate may have been caused by either the Walanae Fault or an unmapped offshore extension of this structure to the SE.

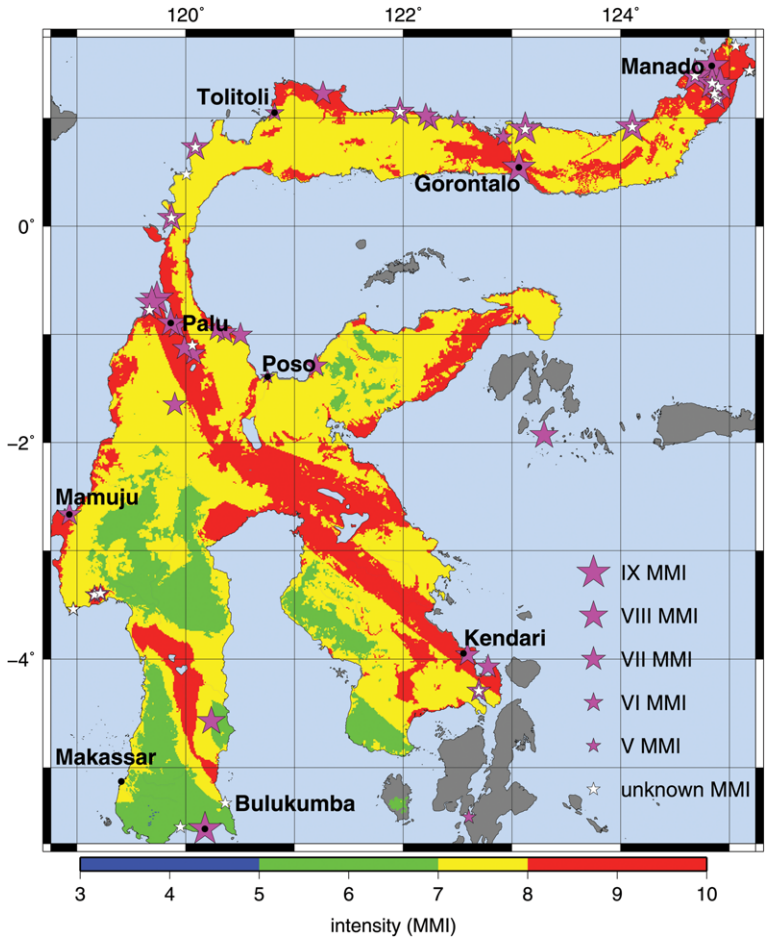

Fig. 8. Intensity map of Sulawesi (500 year recurrence interval 1.0 s) and historical damage location (the size of the star indicates the MMI scale).

A key challenge in developing this hazard map has been reconciling abundant recent seismicity with geological evidence of active structures. With the exception of the Palu-Koro Fault, the geological and geodetic evidence for activity rates is generally weak, while formal uncertainties in earthquake location (Husen & Hardebeck 2010) make attributing specific earthquakes to specific structures problematic. In order to address these issues, large crustal-scale faults that form the boundaries of different domains, such as the Palu-Koro–Matano Fault System, are included as fault sources with their geodetic slip rates and do not overlap background zone sources. Smaller faults that fall within zone sources have their slip rate adjusted to avoid double counting of seismicity. This is done by assuming a volume around the fault and using the seismicity of this volume (based on data in the surrounding source zone scaled to this volume) to calculate the equivalent slip rate for the fault. This is then balanced against the reported slip rate for the fault. In some cases, such as the Poso Fault in north Central Sulawesi, the activity rate estimated from seismicity in the surrounding zone is higher than the estimated slip rate from Irsyam *et al.* (2010). This suggests that the estimated slip rates in Irsyam *et al.* (2010) may be underestimates: however, more detailed geodetic studies are needed to confirm this.

As a result of this approach, hazard results in the northern half of Sulawesi (north of the Palu-Koro–Matano Fault System) are generally high and the role of individual crustal faults in driving the hazard is relatively minor. This is even more so along the northern arm, where subduction interface and intraslab sources contribute significantly

to the hazard, with the effect of the onshore Gorontalo Fault only becoming significant at long return periods (>1000 years). South of this region, and most noticeably in South Sulawesi, background seismicity is lower and seismic activity is concentrated along individual faults, such as the Walanae Fault. Seismic hazard in the central part of Sulawesi is concentrated along the fast-moving Palu-Koro–Matano Fault System and Lawanopo Fault. Several pull-apart basins are present along these fault systems, where sediments have accumulated and resulting in high site amplifications. This is particularly evident near the city of Palu, which sits on a basin of alluvial and coastal sediments bounded to the east and west by two strands of the Palu-Koro Fault.

Palu and Gorontalo are the two most significant population centres located in coastal basins formed by active faulting, although other centres are also in similar situations, including Kendari. These centres are therefore exposed to a combination of high earthquake activity from near-field sources, amplified ground motions, liquefaction and landslide potential, as well as the threat of localized tsunami if earthquake deformation extends offshore or triggers submarine landslides (e.g. tsunami near Palu in 1927 and 1968: Pelinovsky *et al.* 1997). These population centres should be prioritized for more detailed site-amplification studies, hazard assessment for secondary earthquake hazards and risk-reduction activities.

A comparison of our bedrock hazard results with those of Irsyam *et al.* (2010) shows high hazard in the northern part of the island, particular along the north arm, in our assessment (Fig. 9). This may be due to siting the North Sulawesi Subduction Zone source close to the island near the region of most

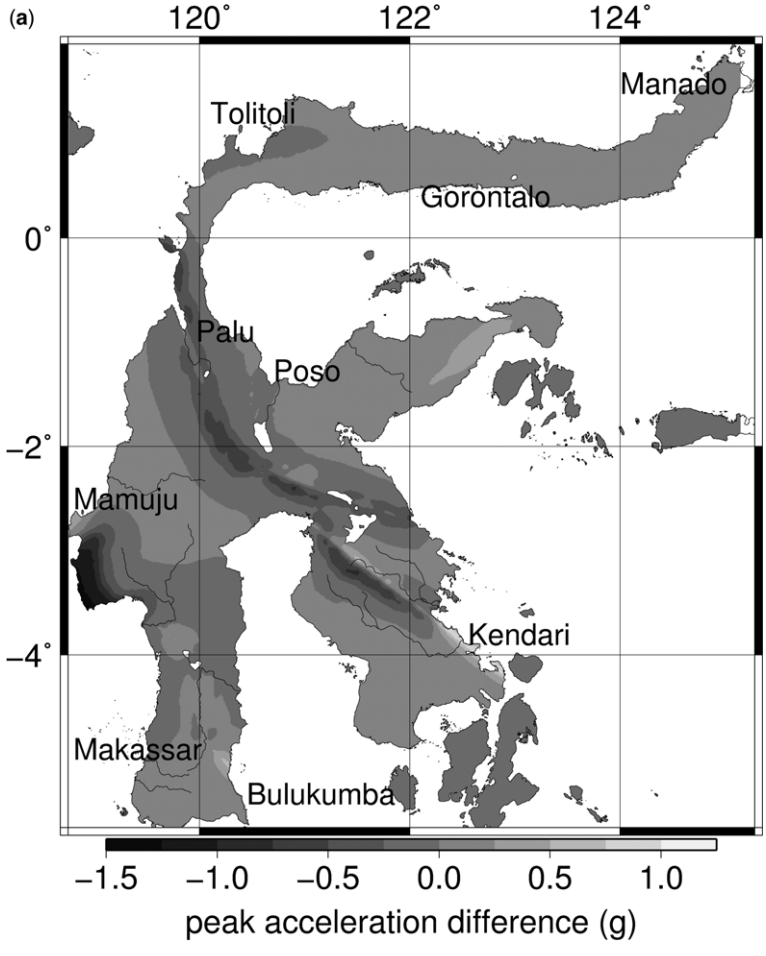

Fig. 9. The PGA difference between the result from this paper and that from Irsyam *et al.* (2010) for (**a**) a 500 year return period.

frequent seismicity, rather than at the trench. We also explicitly include intraslab sources using fault planes with out-of-plane ruptures, allowing us to more realistically capture the geometry of intraslab sources, while Irsyam *et al.* (2010) use smoothed seismicity within stepped rectangular volumes to represent the slab. The Irsyam *et al.* (2010) results are higher along the major crustal faults, including the Palu-Koro–Matano Fault System (Fig. 9).

The assessment presented here uses the same ground-motion prediction equations, and logic tree weightings, as Irsyam *et al.* (2010). None of these GMPEs have been developed using strong-motion data from Indonesia, and therefore there is considerable uncertainty in their application. Analysis of initial data from the newly established Indonesian strong-motion network will begin to reduce uncertainty, although research to date has focused on Java and Sumatra (Rudyanto 2013). Furthermore, the geological heterogeneity of Sulawesi – including thick continenal crust derived from both the Sundaland and Australian continents, overthrust ophiolites and mélange complexes, actively deforming crustal regions, and active and inactive arc systems – means that a high degree of heterogeneity in ground motions is to be expected within Sulawesi.

Proxy methods used to estimate site amplification are subject to considerable uncertainty. The Matsuoka *et al.* (2006) method based on geomorphology is slightly more accurate, correctly classifying site class at approximately 25% of the measured locations compared with the topographical slope method of Wald & Allen (2007), which is correct for approximately 15% of the measured sites. The Wald & Allen (2007) method more accurately assigns site class C, while the Matsuoka *et al.* (2006) method more accurately predicts site class D. Noting the considerable uncertainty in the use of

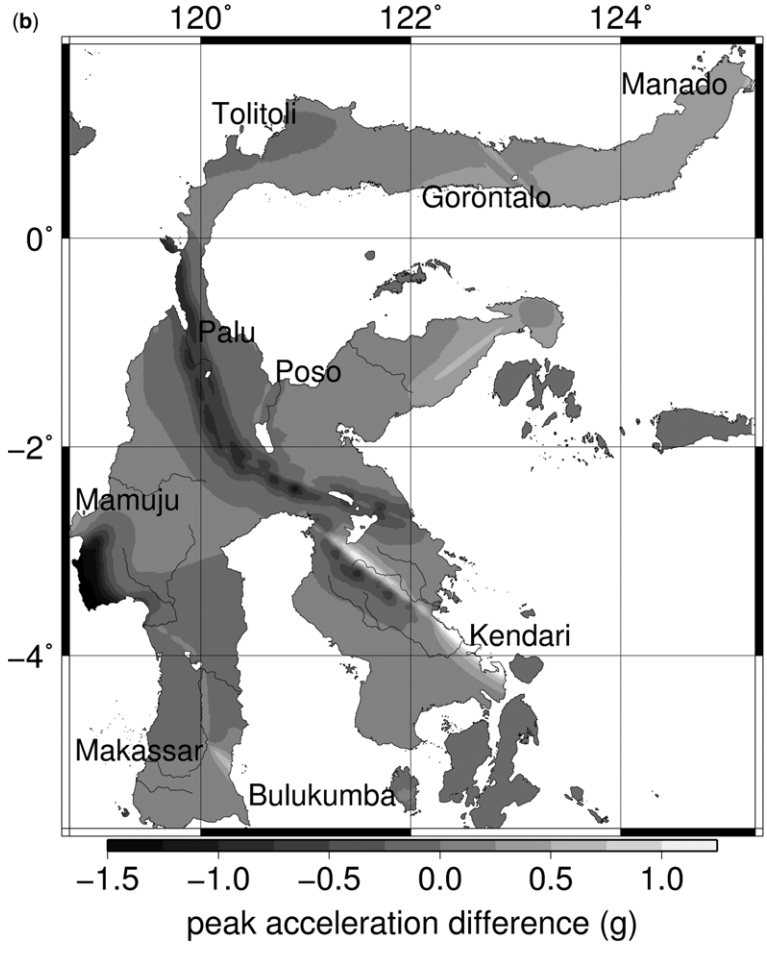

Fig. 9. (**b**) a 2500 year return period.

H/V measurements as a basis for estimating site effects (Ghasemi *et al.* 2009; Zhao 2011), the main conclusion that can be drawn is that the Matsuoka *et al.* (2006) proxy method is probably more suitable for Sulawesi, but that site amplification remains a major source of uncertainty in the hazard results.

By discriminating between volcanic and non-volcanic mountains, the method of Matsuoka *et al.* (2006) is expected to have a distinct advantage over slope-based approaches as there are both active volcanoes and much older non-volcanic mountain regions in Sulawesi. Volcanic product deposited on the footslopes of volcanoes may have low shear-wave velocities (V_{s30} *c.* 200 m s^{-1}), while a terrace covered by volcanic materials may have even lower values (V_{s30} *c.* 160 m s^{-1}) (Matsuoka *et al.* 2006). These geomorphic features, such as footslopes and terraces, are suitable for the deposition of thick loose pyroclastic flow deposits such as ash, pumice and scoria. These deposits have low shear-wave velocities. Low estimates of V_{s30} for areas of active volcanic deposition is consistent with Nunziata *et al.* (1999), who measured shear-wave velocities on recent pyroclastic deposits (younger than 12 000 years) in the Campi-Flegrei caldera (Italy). Although shear-wave velocities were highly variable, they were generally low, varying from less than 200 up to 650 m s^{-1}. Variability in shear-wave velocity of pyroclastic deposits is due to the variability in the materials of particular deposits and the degree of welding that has occurred during diagenesis.

Unfortunately, at present, we do not have any field data with which to test these regions against the Matsuoka *et al.* (2006) classification. Furthermore, many of the major cities are situated in valleys and coastal lowlands and delta. In many cases, these geomorphic environments are a direct result of active faulting in the area, and therefore accurate characterization of site amplification at the local scale will be important for designing critical infrastructure and spatial planning in order to reduce exposure in the areas of greatest amplification. Future field measurements to better understand site amplification should use more robust techniques for calculating site amplification, such as multi-channel analysis of surface waves (MASW), N-SPT (Standard Penetration Test), cone penetration tests (CPT) or borehole measurements. These measurements would be able to validate both the proxy methods and the V_{s30} estimates derived using H/V methods.

Conclusions

A first probabilistic seismic hazard assessment including the effects of site amplification has been undertaken for the island of Sulawesi, Indonesia. Most of the island, with the exception of South Sulawesi, is undergoing rapid deformation, leading to high hazard in most regions (PGA $> 0.4g$ at a 500 year return period including site effects), with extremely high hazard (PGA $> 0.8g$ at a 500 year return period) along fast-slipping crustal-scale faults, such as the Palu-Koro–Matano Fault System and the Lawanopo Fault. Active subduction and a complex array of active and inactive subducted slabs in the north drive very high hazard along the north arm of the island. Reported slip rates for active faults are balanced against background seismicity rates to avoid double-counting seismicity: in many cases, background rates exceed report fault slip rates, highlighting the need for further geodetic and geological studies to better constrain slip rates. Site amplification is included using proxy methods and, combined with conversion to intensity and classification into hazard zones, facilitates use of the hazard maps for spatial planning purposes. A high degree of uncertainty associated with these methods means there is a need for further local-scale studies to better characterize site effects. This is particularly important for the many significant population centres that are sited in sedimentary basins created by currently active faults, including provincial capitals Palu and Gorontalo, and therefore exposed to both high seismicity rates and high amplification of ground motions. Building design in these areas should combine bedrock hazard results with locally measured site effects to determine appropriate design criteria.

The next plan is to try to validate the amplification factor inferred from H/V using a geotechnical approach. Geotechnical investigation, such as N-SPT and CPT, may be a promising method to validate the H/V method to achieve a more reliable amplification factor and, hence, produce a better seismic hazard map.

This work was supported by the Australia Agency for International Development and the Indonesian National Disaster Management Agency through the Australia–Indonesia Facility for Disaster Reduction. The authors are grateful to Masyhur Irsyam (Institut Teknologi Bandung) for sharing input parameters and results from the 2010 revision of the national seismic hazard maps. The authors acknowledge the hard work and fruitful discussions with the EQRM development team (Duncan Gray, Vanessa Newey, David Robinson, Geoscience Australia). We would like to thank Dr Irwan Meilano and the anonymous reviewer for their very useful comments and suggestions.

References

Aki, K. 1965. Maximum likelihood estimate of b in the formula $\log N = a - bM$ and its confidence limits. *Bulletin of the Earthquake Research Institute*, **43**, 237–239.

AMMON, C.J., LAY, T., KANAMORI, H. & CLEVELAND, M. 2011. A rupture model of the 2011 off the Pacific coast of Tohoku earthquake. *Earth, Planets and Space*, **63**, 693–696.

ARIKAN, F. & AYDIN, N. 2012. Research article: influence of weathering on the engineering properties of dacites in Northeastern Turkey. *ISRN Soil Science*, **2012**, article ID 218527. http://doi.org/10.5402/2012/218527

ARYA, A.S., BOEN, T. & ISHIYAMA, Y. 2014. *Guidelines for Earthquake Resistant Non-engineered Construction*. UNESCO.

ATKINSON, G.M. & BOORE, D.M. 2003. Empirical ground-motion relations for subduction-zone earthquakes and their application to cascadia and other regions. *Bulletin of the Seismological Society of America*, **93**, 1703–1729.

ATKINSON, G.M. & KAKA, SL.I. 2007. Relationships between Felt Intensity and Instrumental Ground Motion in the Central United States and California. *Bulletin of the Seismological Society of America*, **97**, 497–510, http://doi.org/10.1785/0120060154

BNPB 2010. *Disaster Data and Information Indonesia*. Badan Nasional Penanggulangan Bencana (Indonesian National Disaster Management Agency), Jakata, http://dibi.bnpb.go.id

BOORE, D.M. & ATKINSON, G.M. 2008. Ground-motion prediction equations for the average horizontal component of PGA, PGV, and 5%-damped PSA at spectral periods between 0.01 sand 10.0 s. *Earthquake Spectra*, **24**, 99–138.

BORCHERDT, R.D. 1994. Estimates of site-dependent response spectra for design (methodology and justification). *Earthquake Spectra*, **10**, 617–653.

BPS 2010. *Population Census of Indonesia*. Badan Pusat-Statistik (Indonesian Central Agency for Statistics), Jakata, http://sp2010.bps.go.id

CAMPBELL, K.W. & BOZORGNIA, Y. 2008. NGA ground motion model for the geometric mean horizontal-component of PGA, PGV, PGD and 5% damped linear elastic response spectra for periods ranging from 0.01 to 10.0 s. *Earthquake Spectra*, **24**, 139–171.

CHIOU, B. & YOUNGS, R. 2008. A NGA model for the average horizontal component of peakground motion and response spectra. *Earthquake Spectra*, **24**, 173–215.

GHASEMI, H., ZARE, M., FUKUSHIMA, Y. & SINAEIAN, F. 2009. Applying empirical methods in site classification, using response spectral ratio (H/V): a case study on Iranian strong motion network (ISMN). *Soil Dynamics and Earthquake Engineering*, **29**, 121–132.

GULICK, S.P., AUSTIN, J.A. JR *ET AL.* 2011. Updip rupture of the 2004 Sumatra earthquake extended by thick indurated sediments. *Nature Geoscience*, **4**, 453–456.

HALL, R. 2011. Australia–SE Asia collision: plate tectonics and crustal flow. *In*: HALL, R., COTTAM, M.A. & WILSON, M.E.J. (eds) *The SE Asian Gateway: History and Tectonics of the Australia–Asia Collision*. Geological Society, London, Special Publications, **355**, 75–109, http://doi.org/10.1144/SP355.5

HANKS, T.C. & KANAMORI, H. 1979. A moment magnitude scale. *Journal of Geophysical Research: Solid Earth*, **84**, 2348–2350.

HUSEN, S. & HARDEBECK, J.L. 2010. Earthquake location accuracy. *Community Online Resource for Statistical Seismicity Analysis*, **10**, http://doi.org/10.5078/corssa-55815573. Available at http://www.corssa.org

IRSYAM, M., SENGARA, W. *ET AL.* 2010. *Development of Seismic Hazard Maps of Indonesia for Revision of Seimic Hazard Map in SNI 03-1726-2002*. Reseach report submitted to the Ministry of Public Works by the Team for Revision of Seismic Hazard Maps of Indonesia.

KOKETSU, K., YOKOTA, Y. *ET AL.* 2011. A unified source model for the 2011 Tohoku earthquake. *Earth and Planetary Science Letters*, **310**, 480–487.

KRAMER, S.L. 1996. *Geotechnical Earthquake Engineering*. Prentice–Hall International Series in Civil Engineering and Engineering Mechanics. Prentice-Hall, Upper Saddle River, NJ.

MATSUOKA, M., WAKAMATSU, K., FUJIMOTO, K. & MIDORIKAWA, S. 2006. Average shear-wave velocity mapping using Japan engineering geomorphologic classification map. *Journal of Structural Mechanics and Earthquake Engineering, JSCE*, **23**, 57–68.

MCCAFFREY, R. & SUTARDJO, R. 1982. Reconnaissance microearthquake survey of Sulawesi, Indonesia. *Geophysical Research Letters*, **9**, 793–796.

NUNZIATA, C., MELE, R. & NATALE, M. 1999. Shear wave velocities and primary influencing factors of Campi-Flegrei_Neapolitan deposits. *Engineering Geology*, **54**, 299–312.

OTTEMÖLLER, V., VOSS, P. & HAVSKOV, J. 2011. *SEISAN Earthquake Analysis Software for Windows, Solaris, Linux and Macosx*, http://www.geosig.com/files//GS_SEISAN_9_0_1.pdf

PELINOVSKY, E., YULIADI, D., PRASETYA, G. & HIDAYAT, R. 1997. The 1996 Sulawesi Tsunami. *Natural Hazards*, **16**, 29–38.

PUSPITA, S.D., HALL, R. & ELDERS, C.F. 2005. Structural styles of the offshore West Sulawesi fold belt, North Makassar Straits, Indonesia. *In*: *Proceedings of the Indonesian Petroleum Association, 30th Annual Convention Jakarta*, August 2005, 519–542.

ROBINSON, D., FULFORD, G. & DHU, T. 2006. *EQRM: Geoscience Australia's Earthquake Risk Model*. Geoscience Australia, Record, 2005/01.

RUDYANTO, A. 2013. *Development of strong-motion database for Sumatra–Java region*. Masters thesis, Australian National University.

SARSITO, D.A., ABIDIN, H.Z., SAPIIE, B., TRIYOSO, W., MEILANO, I. & SIMONS, W.J.F. 2011. Geometric and kinematic modelling of Sulawesi–East Kalimantan zone based on GNSS-GPS and global gravitation data. *Paper presented at the IUGG XXV General Assembly Earth on the Edge: Science for a Sustainable Planet*, Melbourne, Australia, 27 June–8 July 2011.

SCHWARTZ, D.P. & COPPERSMITH, K.J. 1984. Fault behaviour and characteristic earthquakes: examples from the Wasatch and San Andreas fault zones. *Journal of Geophysical Research: Solid Earth*, **89**, 5681–5698.

SILVER, E.A. & MOORE, J.C. 1978. The Molucca Sea Collision Zone, Indonesia. *Journal of Geophysical Research: Solid Earth*, **83**, 1681–1691.

SILVER, E.A., MCCAFFREY, R., JOYODIWIRYO, Y. & STEVENS, S. 1983*a*. Ophiolite emplacement by collision

between the Sula Platform and the Sulawesi island arc, Indonesia. *Journal of Geophysical Research: Solid Earth*, **88**, 9419–9435.

SILVER, E.A., MCCAFFREY, R. & SMITH, R.B. 1983*b*. Collision, rotation, and the initiation of subduction in the evolution of Sulawesi, Indonesia. *Journal of Geophysical Research*, **88**, 9407–9418.

SOCQUET, A., SIMONS, W. *ET AL.* 2006. Microblock rotations and fault coupling in SE Asia triple junction (Sulawesi, Indonesia) from GPS and earthquake slip vector data. *Journal of Geophysical Research*, **111**, B08409.

SPENCER, J.E. 2011. Gently dipping normal faults identified with Space Shuttle radar topography data incentral Sulawesi, Indonesia, and some implications for fault mechanics. *Earth and Planetary Space Science*, **308**, 267–276.

SUPARTOYO & SURONO 2008. *Catalog of Indonesian Destructive Earthquake, Year 1629–2007*. Badan Geologi (Geological Agency of Indonesia), Jawa Barat.

WALD, D.J. & ALLEN, T.I. 2007. Topographic slope as a proxy for seismic site conditions and amplification. *Bulletin of the Seismological Society of America*, **97**, 1379–1395.

WANG, K. & HU, Y. 2006. Accretionary prisms in subduction earthquake cycles: the theory of dynamic Coulombwedge. *Journal of Geophysical Research*, **111**, B06410, http://doi.org/10.1029/2005JB004094

WATKINSON, I.M., HALL, R. & FERDIAN, F. 2011. Tectonic re-interpretation of the Banggai-Sula–Molucca Sea margin, Indonesia. *In*: HALL, R., COTTAM, M.A. & WILSON, M.E.J. (eds) *The SE Asian Gateway: History and Tectonics of the Australia–Asia Collision*. Geological Society, London, Special Publications, **355**, 203–224, http://doi.org/10.1144/SP355.10

YOUNGS, R.R. & COPPERSMITH, K.J. 1985. Implications of fault slip rates and earthquake recurrence models to probabilistic seismic hazard estimates. *Bulletin of the Seismological Society of America*, **75**, 939–964.

YOUNGS, R.R., CHIOU, S.J., SILVA, W.J. & HUMPHREY, J.R. 1997. Strong ground motion attenuation relationships for subduction zone earthquakes. *Seismological Research Letters*, **68**, 58–73.

ZHAO, J.X. 2011. Comparison between VS30 and site period as site parameters in ground-motion prediction equations for response spectra. *Paper presented at the 4th IASPEI/IAEE International Symposium: Effects of Surface Geology on Seismic Motion*, Santa Barbara, California, 23–26 August 2011.

ZHAO, J.X., ZHANG, J. *ET AL.* 2006. Attenuation relations of strong motion in Japan using site classification based on predominant period. *Bulletin of the Seismological Society of America*, **96**, 898.